Multiscale control and rapid scanning of time delays ranging from picosecond to millisecond

Xavier Solinas, Laura Antonucci, A. Bonvalet, Manuel Joffre

Research Article | Vol. 25, No. 15 | 24 Jul 2017 | OPTICS EXPRESS 17811
Optics EXPRESS

Multiscale control and rapid scanning of time delays ranging from picosecond to millisecond

XAVIER SOLINAS, LAURA ANTONUCCI, ADELINE BONVALET, AND MANUEL JOFFRE*

Laboratoire d'Optique et Biosciences, Ecole Polytechnique, CNRS, INSERM, Université Paris-Saclay, 91128 Palaiseau, France
manuel.joffre@polytechnique.edu

Abstract: Femtosecond amplifiers seeded by two independent femtosecond oscillators normally produce amplified pulse pairs with a timing jitter equal to the oscillator period, which is typically around 12 ns for Titanium:Sapphire lasers. Combining Arbitrary-Detuning Asynchronous Optical Sampling (AD-ASOPS) with an appropriate selection of amplified pulses, we demonstrate that the time-delay distribution can be narrowed down to a 25-ps time window, allowing to produce spectral interference fringes for each amplified pulse pair. Subsequent AD-ASOPS determination of the actual time delay with subpicosecond accuracy allows to tailor the delay distribution with an electronic control all the way to the repetition period of the amplifiers. We thus demonstrate rapid scanning of the time delays up to nearly 1 ms with a sub-picosecond accuracy, which makes this method an ideal tool for multiscale pump-probe spectroscopy.

OCIS codes: (320.7100) Ultrafast measurements; (320.7160) Ultrafast technology; (320.7120) Ultrafast phenomena.

References and links

1. G. Sucha, M. E. Fermann, D. J. Harter, and M. Hofer, "A new method for rapid temporal scanning of ultrafast lasers," IEEE J. Sel. Top. Quant. Electr. **2,** 605–621 (1996).
2. J. Bredenbeck, J. Helbing, J. R. Kumita, G. A. Woolley, and P. Hamm, "Alpha-Helix formation in a photoswitchable peptide tracked from picoseconds to microseconds by time-resolved IR spectroscopy," Proc. Natl. Acad. Sci. USA **102,** 2379–2384 (2005).
3. M. M. Leonova, T. Y. Fufina, L. G. Vasilieva, and V. A. Shuvalov,"Structure-function investigations of bacterial photosynthetic reaction centers," Biochemistry (Mosc) **76,** 1465–1483 (2011).
4. L. Antonucci, A. Bonvalet, X. Solinas, M. R. Jones, M. H. Vos, and M. Joffre, "Arbitrary-detuning asynchronous optical sampling pump-probe spectroscopy of bacterial reaction centers," Optics Letters **38,** 3322–3324 (2013).
5. E. Lill, S. Schneider, and F. Dorr, "Rapid optical sampling of relaxation-phenomena employing 2 time-correlated picosecond pulsetrains," Appl. Phys. **14,** 399–401 (1977).
6. P. A. Elzinga, F. E. Lytle, Y. Jian, G. B. King, and N. M. Laurendeau, "Pump probe spectroscopy by asynchronous optical-sampling," Appl. Spectrosc. **41,** 2–4 (1987).
7. J. D. Kafka, J. W. Pieterse, and M. L. Watts, "2-color subpicosecond optical-sampling technique," Opt. Lett. **17,** 1286–1288 (1992).
8. F. Keilmann, C. Gohle, and R. Holzwarth, "Time-domain mid-infrared frequency-comb spectrometer," Opt. Lett. **29,** 1542–1544 (2004).
9. R. Gebs, G. Klatt, C. Janke, T. Dekorsy, and A. Bartels. "High-speed asynchronous optical sampling with sub-50fs time resolution," Opt. Express **20,** 5974–5983 (2010).
10. H. R. Ma, J. Ervin, and M. Gruebele, "Single-sweep detection of relaxation kinetics by submicrosecond midinfrared spectroscopy," Rev. Sci. Instr. **75,** 486–491 (2004).
11. J. Bredenbeck, J. Helbing, and P. Hamm, "Continuous scanning from picoseconds to microseconds in time resolved linear and nonlinear spectroscopy," Rev. Sci. Instr. **75,** 4462–4466 (2004).
12. A. C. Yu, X. Ye, D. Ionascu, W. X. Cao, and P. M. Champion, "Two-color pump-probe laser spectroscopy instrument with picosecond time-resolved electronic delay and extended scan range," Rev. Sci. Instr. **76,** 114301 (2005).
13. L. Antonucci, X. Solinas, A. Bonvalet, and M. Joffre, "Asynchronous optical sampling with arbitrary detuning between laser repetition rates," Opt. Express **20,** 17928–17937 (2012).
14. L. Antonucci, A. Bonvalet, X. Solinas, L. Daniault, M. Joffre, "Arbirary-detuning asynchronous optical sampling with amplified laser systems," Opt. Express **23,** 27931–27940 (2015).
15. T. Nakagawa, K. Okamoto, H. Hanada, and R. Katoh, "Probing with randomly interleaved pulse train bridges the gap between ultrafast pump-probe and nanosecond flash photolysis," Opt. Lett. **41**, 1498–1501 (2016).
16. F. Reynaud, F. Salin, and A. Barhtelemy, "Measurement of phase shifts introduced by nonlinear optical phenomena on subpicosecond pulses," Opt. Lett. **14,** 275–277 (1989).

#296905 https://doi.org/10.1364/OE.25.017811
Journal © 2017 Received 26 May 2017; revised 6 Jul 2017; accepted 6 Jul 2017; published 17 Jul 2017

Optics EXPRESS

17. L. Lepetit, G. Chériaux, and M. Joffre, "Linear techniques of phase measurement by femtosecond spectral interferometry for applications in spectroscopy," J.Opt. Soc. Am.B. **12,** 2467–2474 (1995).
18. C. Dorrer, N. Belabas, J.-P. Likforman, and M. Joffre, "Spectral resolution and sampling issues in Fourier-transform spectral interferometry," J. Opt. Soc. Am. B **17,** 1795–1802 (2000).

1. Introduction

Femtosecond pump-probe spectroscopy is one of the most widespread techniques for investigating the ultrafast dynamics of numerous systems in physics, chemistry and biology. In a typical pump-probe experiment, the laser beam delivered by a single femtosecond laser is split in two beams, one of which – the pump – triggers a time-dependent process analyzed using the second beam – the probe. The relative delay between these two pulses, called the pump-probe delay, is most often controlled by varying the optical path of one of the beams with respect to the other using a translation stage. For practical reasons related to the length of the required optical path [1], using such a mechanical delay line limits the maximum delay to a few nanoseconds. However, many systems of interest, such as complex biomolecules, exhibit a multiscale distribution of time constants, from hundreds of femtosecond up to milliseconds [2–4].

Several methods have been designed in order to meet the challenge of covering such a huge time range. The key point for increasing accessible time delays is to generate the pump and probe pulses from two different lasers. One such method, ASynchronous OPtical Sampling (ASOPS) [5–9], relies on two oscillators of repetition frequencies f_1 and f_2 taking slightly different values. The pump-probe delay is thus varied at a scanning rate $\Delta f = f_2 - f_1$ over a time interval $T_1 = 1/f_1$ corresponding to the repetition period of the pump oscillator (around 12 ns for typical Titanium:Sapphire oscillators). Much longer pump-probe delays have been achieved by using a pump laser running at a lower repetition rate, albeit with nanosecond pump pulses in the initial demonstration [10]. Finally, covering the picosecond to millisecond time range was made possible with the two-amplifier method, which relies on two femtosecond amplifiers seeded by two phase-locked oscillators of identical repetition rates [11, 12]. Fine tuning of the time delay was then achieved by adjusting the relative phase between the pulse trains of the two oscillators, whereas coarse tuning was achieved by T_1 steps through electronic control of the amplifier trigger signals. The time delay can thus be scanned all the way up to the amplifier repetition period, *i.e.* 1 ms for typical 1-kHz amplifier systems. However, as this method requires a servo loop acting on the cavity length of one of the two oscillators, its implementation on pre-existing femtosecond amplified systems is not entirely straightforward.

By combining Arbitrary Detuning ASynchronous OPtical Sampling (AD-ASOPS) [13] with the two-amplifier method, we have recently demonstrated the so-called kHz AD-ASOPS method [14]. Coarse tuning was achieved similarly to the conventional two-amplifier method, while fine tuning was replaced with an *a posteriori* determination of the time delays of amplified pulses allowing to average pump-probe data in appropriate time bins. Indeed, using AD-ASOPS, it is possible to determine with a sub-picosecond accuracy the law of variation

$$\Delta t_i = (a\, i + b)\ [T_1] \tag{1}$$

of the time delay between pulse pairs produced by the oscillators seeding the two amplifiers, where i is the pulse number in the pulse train produced by the probe oscillator and $[T_1]$ stands for the modulo-T_1 operation. The slope a (equal to $(T_2 - T_1)[T_1] = T_2[T_1]$) and the offset b were continuously tracked as described previously [13] in order to account for variation in the lengths of the oscillator cavities. Note that, in contrast with the recently-reported Randomly Interleaved Pulse Train (RIPT) method [15], the AD-ASOPS method is not limited by the time resolution of electronic detectors because it takes advantage of the remarkable clock stability of the oscillators, thus permitting sub-picosecond accuracy. Once the law associated with eq. 1 is known, it is

Optics EXPRESS

straightforward to determine *a posteriori* the time delay between amplified pulses simply from the knowledge of the number i of the oscillator pulse that was amplified.

Since there is no requirement on the repetition rates of the two oscillators (apart from the fact that they should not be identical or related by a rational number with a too-small denominator), the kHz AD-ASOPS method can be easily implemented on existing amplifiers by the mere addition of an opto-electronic device. However, in our first implementation [14], there was no active control of the time delay on a sub-T_1 timescale. Indeed, due to the use of independent free-running oscillators, the timing jitter between the two oscillators resulted in time delays uniformly distributed in a time window of width equal to T_1. Although the sub-picosecond accuracy in time delay was still preserved thanks to the *a posteriori* AD-ASOPS determination, this effect can be a major issue in terms of signal to noise ratio. Indeed, in a typical multiscale pump-probe measurement, it is usually desired to acquire the data with time steps arranged on a logarithmic time scale. As a result, the width of time bins varies exponentially with time delay. In case of a uniform distribution of achieved time delays, the number of accumulated pulses will be exponentially smaller for time bins associated with short delays. This results in a greater noise for smaller delays, as observed for example in Fig. 3 of reference [4]. Although this problem remains minor in case of higher repetition-rate experiment, it is quite detrimental for pump-probe experiments performed with the smaller repetition rates associated with amplified laser systems.

In this article, we demonstrate an improved kHz AD-ASOPS method where this latter drawback is entirely overcome. This can be achieved thanks to the fact that amplified pulses do not need to be perfectly equally spaced in the oscillator pulse trains, so that we can take advantage of an additional degree of freedom. Indeed, by an appropriate choice of the pulses to be amplified, we demonstrate that the timing jitter between amplified pulses can be reduced by almost three orders of magnitude, while preserving the sub-picosecond accuracy in the knowledge of the time delay between amplified pulses. It thus becomes possible to tailor the time delay distribution at will and to generate for example an exponential distribution of time delays as desired in a typical multiscale pump-probe measurement. As an additional benefit, we demonstrate that our approach makes rapid scanning straightforward even with an arbitrary time delay distribution, in contrast with previously-reported multiscale methods.

2. Deterministic control of the pump-probe time delay

Figure 1 shows the experimental setup required for applying the kHz AD-ASOPS method using a combination of two femtosecond amplifiers seeded by two independent free-running oscillators. We use two commercial Titanium:Sapphire amplified systems, the Hurricane (Spectra-Physics) and Libra-HE (Coherent) including integrated oscillators, the Mai-Tai (Spectra-Physics) and Vitessse (Coherent), respectively. Their repetition rates, $f_1 \approx 79916$ kHz and $f_2 \approx 80107$ kHz, differ by a value $\Delta f = f_2 - f_1 \approx 191$ kHz. As described previously [13, 14], a fraction of the two oscillator beams is collected by the so-called AD-ASOPS device which detects time coincidences between the two oscillators using a fiber-based optical interferometer and balanced detection. The AD-ASOPS electronics, which includes a commercial development card with a Spartan 6 FPGA SP601 (Xilinx) and a fast home-made I/O card, counts for each oscillator the number of pulses elapsed between coincidences, so that parameters a and b (see eq. 1) can be regularly updated. In practice, each time a coincidence associated with pulse number i is detected, b is reset according to eq. 1 to the value $-a\,i$, whereas a is adjusted from the period ratio $T_2/T_1 \approx N_1/N_2$, where N_1 and N_2 are the number of pulses elapsed since the previous coincidence for each oscillator [13]. The electronics also generates trigger signals (Trig1 and Trig2) in order to fire the two amplifiers with an appropriate coarse control of the time delay. In the mode of operation that we previously reported [14], the repetition rate of the amplifiers was set to 1 kHz by counting exactly 80107 pulses from oscillator #2 between trigger signals (see time diagram in Fig. 2). As discussed above, the sawtooth variation of the time delay Δt_i

Optics EXPRESS

between oscillator pulses then results in a homogeneous distribution of pump-probe delays over a width $T_1 = 1/f_1 \approx 12.5$ ns.

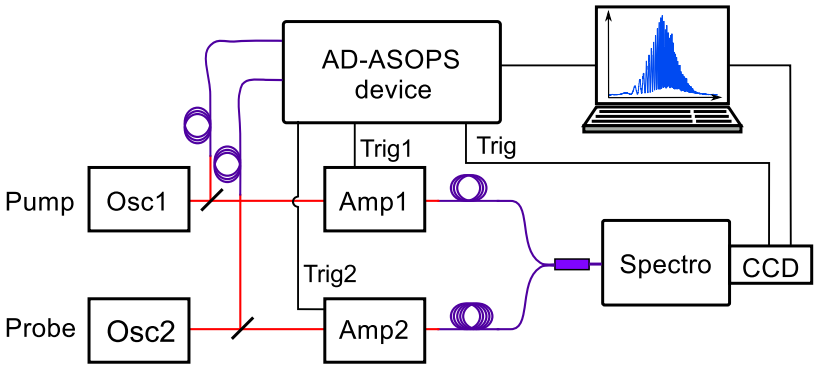

Fig. 1. Experimental setup. Two independent free-running Titanium:Sapphire oscillators (Osc1 and Osc2) seed two Titanium:Sapphire amplifiers (Amp1 and Amp2). A small fraction of the two oscillator pulse trains is collected by the AD-ASOPS device in order to compute time delays in advance and accordingly generate suitable trigger signals firing the amplifiers. The pump and probe pulses are sent into a fiber-based interferometer producing spectral fringes measured using a spectrometer and CCD camera. Note that the interferometer dispersion is intentionally unbalanced by using a longer optical fiber in the probe arm so that the resulting spectral fringes are sensitive to the sign of the time delay.

Our new kHz AD-ASOPS method takes advantage of the fact that femtosecond amplifiers can tolerate a moderate shot-to-shot fluctuation in repetition period. As shown in Fig. 2, by allowing a $\pm\delta T/2$ variation in the delay between amplified pulses, one can choose the best pulse to be amplified among a set of $f_2\delta T$ possible candidates associated with different values of the time delay. Aiming at a reduction of about three orders of magnitude in timing jitter, we need to benefit from a set of 1000 pulses, associated with $\delta T = 1000/f_2 \approx 12.5\ \mu$s. This value

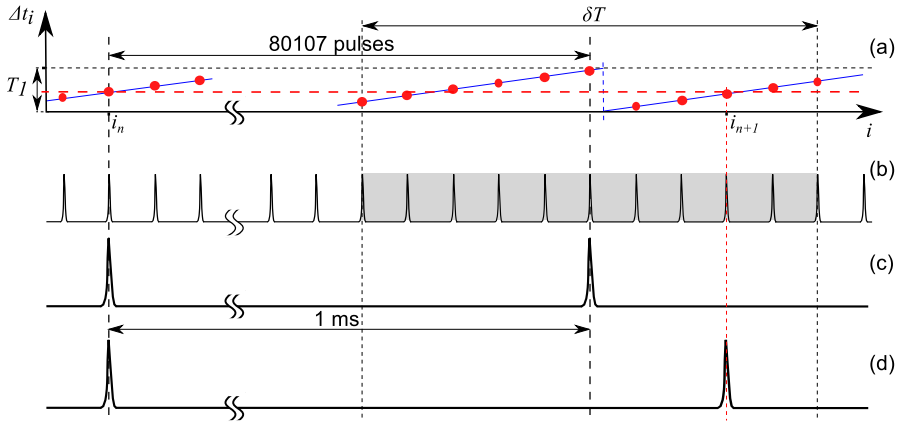

Fig. 2. Schematic time diagram showing (a) the sawtooth variation of the time delay Δt_i, (b) the probe oscillator pulse train, (c) equally spaced amplified probe pulses found in conventional amplifiers and (d) amplified probe pulses with a pump-probe delay close to the target value (horizontal dashed red line in (a)) by allowing a δT tolerance in repetition period (shaded area in (b)).

Optics EXPRESS

corresponds to a ±0.6% variation in repetition rate which turned out to be well tolerated by both amplifiers. Note that the detuning Δf between the two oscillators must be large enough so that the entire T_1 window is scanned at least once during the interval δT. This requirement translates into the condition $|\Delta f| \geq 1/\delta T = 80\,\text{kHz}$, which is indeed fulfilled with our own oscillators ($\Delta f = 191\,\text{kHz}$). In practice, immediately after firing amplified pulse number n, the FPGA starts performing the required computations for preparing trigger signals associated with the next amplified pulse, $n+1$, which is to take place roughly 1 ms later. Let us call i_n the number in the probe oscillator pulse train that was just amplified, and i_{n+1} the number we need to determine associated with the best candidate to be amplified next. Using eq. 1, the FPGA computes all 1000 time delays $\Delta t_i = (a\,i + b)[T_1]$ for $i \in [i_n + 79607, i_n + 80606]$, corresponding to a window of width δT centered 1 ms after the pulse amplified previously (shaded area in Fig. 2(b)). Among this set, the FPGA determines the index i_{n+1} associated with the result closest to the target value Δt needed for fine tuning of the pump-probe delay. Thanks to an efficient implementation of this algorithm in the FPGA using VHDL (VHSIC - Very High Speed Integrated Circuit - Hardware Description Language), the entire computation for the 1000 candidate pulses takes only 5 μs, so that the FPGA is ready well in advance to generate trigger signals for both amplifiers that will be needed roughly 1 ms later. The process is then repeated for subsequent amplified pulses.

In order to demonstrate proper operation of this new method, we use a photodiode (PDB130A-AC, Thorlabs) to monitor the amplified pulses using a 1-GHz oscilloscope (WaveSurfer 104MXs-A, Lecroy) triggered on the Trig2 signal. In the old mode of operation, we observe that amplified pump pulses exhibit the expected 12.5-ns jitter. But when we switch to the improved algorithm, we observe that the jitter is no longer visible on the oscilloscope and that the two amplified pulses appear perfectly locked. We also checked that both coarse and fine tuning of the pump-probe time delay could be readily achieved. In order to evaluate the residual pump-probe jitter, we first rely on the AD-ASOPS method itself for computing the time delays of amplified pulses. In a set of 250000 consecutive amplified pulses, we observe that 92.6% of all pulses fall within a 25-ps window, whereas only 59.9% fall within a window of width 15 ps. If the 1000 candidate pulses were uniformly distributed in a window of width equal to T_1, we would have naively expected to obtain a reduction in jitter by a factor of 1000 (12.5 ps), instead of the factor of about 500 observed experimentally (25 ps). We attribute this result to the fact that the oscillator frequencies happen to fall in a case where consecutive scans do not explore sufficiently different values of the time delay. In practice, the reduction in timing jitter will depend on the exact values of the ratio $f1/f2$ and will sometimes be less important when this ratio falls too close to a rational number with a small denominator.

3. Measurement of the time delays using spectral interferometry

We now turn to an independent method, based on spectral interferometry [16], for measuring the time delays between amplified pulses. As shown in Fig. 1, amplified pump and probe pulses are recombined in a fiber-based interferometer and spectrally resolved using a 0.5-m SpectraPro 2500i spectrometer (Acton, Princeton Instruments). Individual spectra are measured at 1 kHz using a CCD camera (Spec-10 100F, Roper Scientific) externally triggered by the AD-ASOPS device. Spectra can thus be numbered by the acquisition software starting with $n = 1$ associated with the first trigger signal, so that the AD-ASOPS device can transmit appropriate values of a, b and oscillator pulse number i_n for each amplified pulse n. This allows to attribute the appropriate AD-ASOPS delay to each measured spectrum in the experiment described below, or for averaging each acquired spectrum in the appropriate time bin in the case of an actual pump-probe experiment.

Using the kHz AD-ASOPS method described in the previous section, we adjust the pump-probe target time delay in order to minimize the delay between the two pulses in the interferometer. Figure 3(a) shows experimental spectra thus recorded for 50 consecutive laser shots. In marked

Optics EXPRESS

contrast with our previous work, where the occurrence of spectral interferences between amplified pulses was a rare event as the fringes were most often too narrow to be resolved [14], we now observe spectral interference fringes for each amplified pulse pair. In itself, this is a quite remarkable result : two independent amplifiers, seeded by two independent free-running oscillators, are made to interfere in a spectrometer for each laser shot, provided appropriate oscillator pulses are selected for amplification.

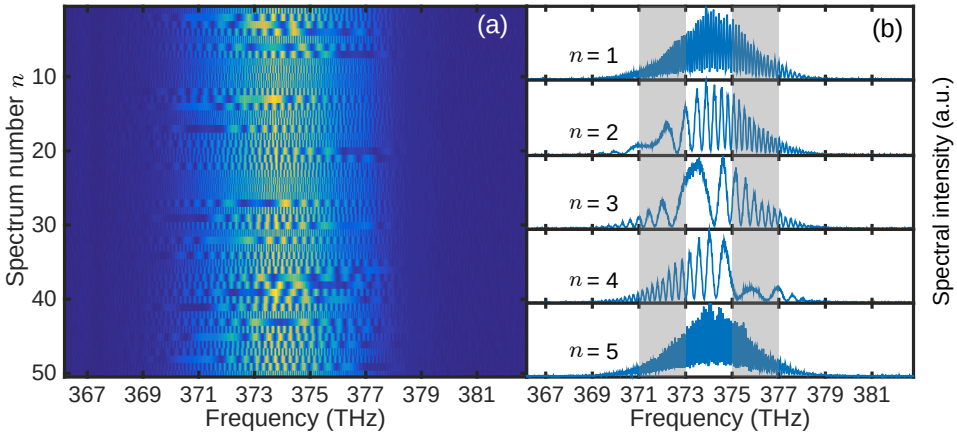

Fig. 3. (a) Interference spectra measured for 50 consecutive amplified laser shots. (b) Interference spectra associated with the first 5 pulses of the previous set, associated with retrieved pump-probe delays (defined at a center frequency $\omega_0/(2\pi) = 374\,\text{THz}$) equal to -8.91, 3.07, 0.98, -2.00 and -12.02 ps.

Figure 3(b) shows individual spectra associated with the first five shots. For the first laser shot ($n = 1$), the fringe spacing is observed to increase as the frequency increases, evidencing a smaller delay for greater frequencies. Considering the differential dispersion of the interferometer, this behavior indicates that the probe pulse arrives on the interferometer before the pump pulse, hence corresponding to a negative pump-probe delay. Using Fourier-Transform Spectral Interferometry (FTSI) [17, 18] and a second-order polynomial fit, we can extract the spectral phase and retrieve a pump-probe delay of -8.91 ps (as defined from the slope of the spectral phase at a frequency of 374 THz) and a second-order differential spectral phase $\varphi'' \approx 0.16\,\text{ps}^2$. As in our previous work [14], subsequent spectra can be processed by subtracting (or adding, depending on the sign of the delay) the quadratic spectral phase $(1/2)\varphi''(\omega - \omega_0)^2$ and performing a linear fit on the phase difference to retrieve the time delay. This standard FTSI processing is known to fail when the time delay is too small, which happens to be the case for three of the spectra ($n = 2, 3, 4$) shown in Fig. 3(b). To avoid such a gap around zero delay, we improve our numerical processing by defining two spectral areas centered around frequencies 372 and 376 THz (shown as shaded areas in Fig. 3(b)) and applying the FTSI procedure selectively in each area. Thanks to the differential dispersion, the actual delays at 372 and 376 THz differ by $0.16 \times 2\pi \times 4 \approx 4$ ps, so that at least one of the two areas is suitable for FTSI processing. For example, spectra associated with $n = 2$ and $n = 3$ can be processed using the higher-frequency area (yielding delays equal to 3.07 and 0.98 ps respectively), while the spectrum associated with $n = 4$ can be processed using the lower-frequency area, yielding a delay of -2.00 ps. This advanced FTSI processing can be easily automated, allowing a determination of the time delay with no gap around zero delay.

Figure 4(a) shows a histogram of the time delays measured using the advanced FTSI method described above. In agreement with the results discussed in the previous section, the pump-probe delays are distributed over a region of width roughly equal to 25 ps. Figure 4(b) shows the

Optics EXPRESS

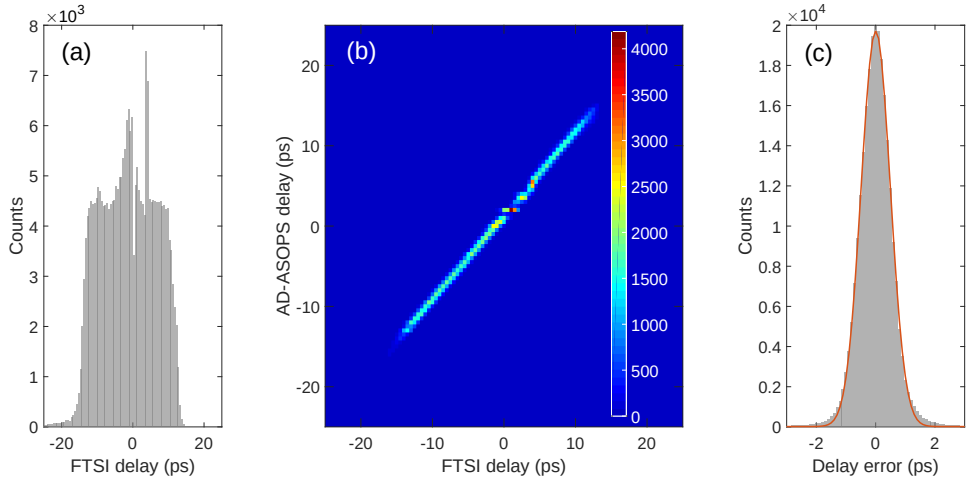

Fig. 4. (a) Histogram of the time delay retrieved using the FTSI procedure described in the text, for a total of 250000 laser shots. The bin size is 0.5 ps. (b) Correlation plot of the time delays retrieved using AD-ASOPS and FTSI (time bins of 0.5 × 0.5 ps). (c) Histogram of the time difference between AD-ASOPS and FTSI (time bins of 0.1 ps). The red curve is a gaussian fit corresponding to a standard deviation of 0.49 ps.

correlation between AD-ASOPS and FTSI measurement of the time delays, while Fig. 4(c) shows the histogram of the difference between the two measurements. We obtain an excellent agreement between the two methods for determining the time delay, with a standard deviation of 0.49 ps. This confirms our previous work establishing the validity of the kHz AD-ASOPS measurement [14], except that we are dealing here with a much greater number of useful data points thanks to the 500-fold reduction in pump-probe jitter.

4. Application to rapid scanning

A unique feature of our method is that the time delay distribution can be tailored at will with only a few constraints as compared to other methods. While ASOPS permits high scanning rates thanks to the absence of moving parts, the time delay thus produced assumes a linear variation with respect to time, resulting in a homogeneous time delay distribution. In contrast, thanks to the selection of pulses of interest, kHz AD-ASOPS provides great agility in time delay control, with only two limiting factors. First, changing the time delay is limited by a maximum slew rate related to the tolerance $\delta T = 12.5\ \mu$s introduced above on the maximum variation in amplifier repetition period. Thus, it will not be possible to change the pump-probe delay by an amount greater than δT between consecutive amplified pulses, *i.e.* a slew rate of 12.5 μs/ms (corresponding to one amplifier running at 993.8 Hz and the other one at 1006.3 Hz). The second limitation associated with our method is that control of the time delay is deterministic only down to 25 ps. Below this value, time delays will be randomly distributed.

To illustrate the unique agility of kHz AD-ASOPS, we program our device in order to generate a time delay distribution typical of a multiscale pump-probe experiment, with a time axis plotted in linear scale close to zero delay and in logarithmic scale for longer delays. Our target time delay distribution $\{\tau_n\}$ thus consists of two regions. In the first region ($n \in [1, 101]$), we have a homogeneous distribution of 101 time bins of 1-ps width covering the [0, 100 ps] time interval, in order to measure the vicinity of the pump-probe overlap with a time resolution comparable to that of our method. Second, for $n \in [102, N + 101]$ (with $N = 1194$), the delay spans the interval

Optics EXPRESS

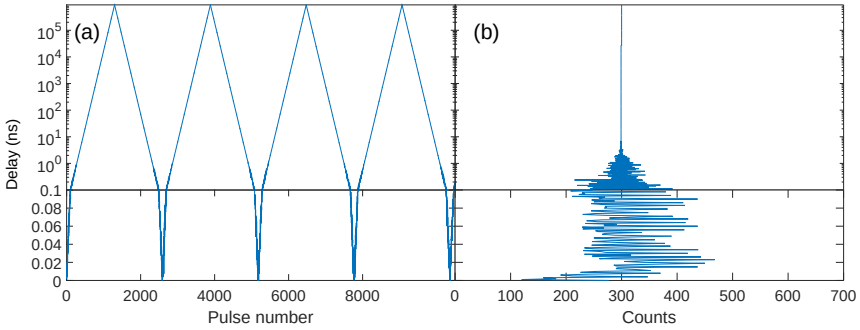

Fig. 5. Demonstration of a delay profile homogeneously distributed in [0,100 ps] time interval (linear scale) and in [101 ps, 900 μs] time interval (logarithmic scale). (a) AD-ASOPS time delay measured as a function of pulse number, with an ascending and descending distribution of period equal to 2590 pulses (or 2.59 s). (b) Histogram of time delays after averaging for 150 periods (corresponding to 388500 laser shots).

[101 ps, 900 μs] using an exponential distribution of time delays

$$\tau_n = \tau_{\min} \exp\left(\frac{n-102}{N-1} \ln \frac{\tau_{\max}}{\tau_{\min}}\right) \tag{2}$$

with $\tau_{\min} = 101$ ps and $\tau_{\max} = 900\,\mu$s. Note that the maximum time step, corresponding to the difference between the last two delays, is roughly equal to 12 μs – indeed smaller than the limit value $\delta T = 12.5\,\mu$s. The delay is then decreased down to zero in a symmetric fashion. Figure 5(a) shows the time delay measured using AD-ASOPS with this time-delay profile, repeated periodically with a period of 2590 laser shots. This corresponds to an acquisition time period of 2.59 s, which is a remarkably short duration for scanning such a broad time range. Figure 5(b) shows the histogram of actual time delays after averaging for 150 periods, *i.e.* 388.5 s. The fact that for small time delays the number of counts per time bin deviates from the average value of 300 is a signature of the not-entirely deterministic control of the time delay, with a residual jitter of 25 ps. However, it is clear that this effect is not detrimental to a pump-probe measurement as the averaged pump-probe data is normalized taking into account the appropriate number of laser shots associated with each time bin. The important issue here is that all time bins are reasonably well populated, thanks to the 500-fold reduction in timing jitter.

Figure 6 shows an even more rapid scanning, with only ten different target values of the time delay extending up to 10 μs. The delay profile is repeated with a period of 20 laser shots, corresponding to a scanning rate of 50 Hz. Switching between two different delays could be similarly achieved at a rate of 500 Hz, in order to perform a lock-in detection based on the difference between two specific time delays (although in this case the time resolution would be limited to 25 ps).

5. Conclusion

To summarize, we demonstrate that the timing jitter between two femtosecond amplifiers seeded by two independent free-running oscillators can be reduced by a large amount, roughly equal to 500 in our experimental conditions. This is achieved by allowing a small fluctuation in the repetition period of the two amplifiers, making possible the selection of pairs of oscillator pulses to be amplified with a relative time delay closest to a target value set by the user. This selection is performed by fast electronics able to compute the time delay between candidate pulse pairs using the Arbitrary-Detuning ASynchronous Optical Sampling (AD-ASPOS) method. In order to remain on the safe side of the amplifier specifications and to preserve the stability of the

Optics EXPRESS

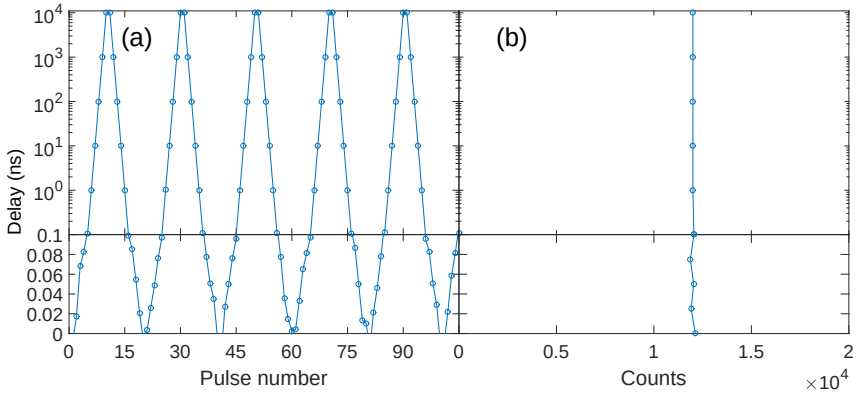

Fig. 6. Rapid scanning at 50 Hz with only 10 time delays : 0, 25, 50, 75, 100 ps, 1, 10, 100, 1000, 10000 ns. (a) Time delays actually achieved as measured using AD-ASOPS. (b) Histogram of time delays accumulated after an accumulation time of 120 s.

amplified pulses, we chose to use a very small value of the allowed fluctuation in repetition rate (±0.6 %), although much greater reduction in timing jitter should be achievable by allowing greater fluctuation. Conversely, for a given percentage in allowed fluctuation, the number of candidate pulses will be smaller for femtosecond amplifiers with greater values of the repetition rate, resulting in a smaller reduction of timing jitter.

As a consequence of the small value of the remaining timing jitter (25 ps), the femtosecond pulses delivered by our two amplifiers generate resolvable spectral interferences for each pair of laser shots, even though these pulses originate from two independent free-running oscillators. Thanks to the use of an interferometer with unbalanced dispersion and of an advanced processing of the spectral fringes, we are able to retrieve the time delay – including its sign – with no gap around zero delay. The AD-ASOPS determination of the time delay is thus independently validated by the comparison with spectral interferometry. The standard deviation between the two methods is 0.5 ps, in agreement with our previous work on AD-ASOPS.

Our method constitutes an ideal tool for multi-timescale pump-probe spectroscopy from picosecond to millisecond, as it can be readily implemented on a set of two pre-existing femtosecond amplifiers. The time delay distribution can be tailored according to experimental needs, with for example a homogeneous distribution around zero time delay and an exponential distribution – suitable for a logarithmic time scale – for longer time delays. We stress that, in this context, the remaining uncertainty of 25 ps in the control of time delay is not detrimental to the experiment : for short delays, the quasi-random distribution of time delays thus produced is appropriate for filling a nearly-homogenous distribution of time bins, whereas for longer delays the uncertainty in time delay control becomes negligible with respect to the bin size. Finally, we emphasize that a unique feature of our method is that it permits rapid scanning of time delays, even in the case of an exponential delay distribution.

Funding

LabEx PALM (“Investissement d’avenir” program ANR-10-LABX-0039-PALM).